

Noise of a single-ion frequency standard

Peter E. TOSCHEK *
 Bernd APPASAMY *
 Philippe COURTEILLE *
 Ralf HUESMANN *
 Yves STALGIES *

Abstract

A frequency source supposed to serve as a standard requires feedback for short-term and long-term frequency control. A spectral discriminant for short-term control may be provided, in the microwave regime, by a hyperfine resonance of a multi-ion ensemble confined in an electrodynamic trap, and in the optical regime by an eigenmode of a focal Fabry-Pérot cavity. For long-term frequency control, resonances of single trapped ions are discriminants of superior accuracy although the controlled frequency shows random fluctuations caused by noise on the feedback signal. Its fundamental contribution is quantum projection noise. The detection of fluorescence for the generation of feedback is incompatible with the ions being prepared in a superposition state in the excitation by the wave emitted from the oscillator. Attempts of circumventing this limitation by preparing ensembles of correlated ions prior to the measurement (spin squeezing) are reviewed.

Key words : Frequency standard, Frequency control, Optical resonator, Short term, Long term, Frequency stability, Ion trapping, Multiple resonance, Quantum effect.

BRUIT D'UN ÉTALON DE FRÉQUENCE À ION UNIQUE

Résumé

Une source de fréquence destinée à servir d'étalon nécessite une rétroaction pour la commande à court et long terme de la fréquence. Un discriminateur spectral pour la commande à court terme peut être fourni, dans le régime microondes, par une résonance hyperfine d'un

ensemble multiionique confiné dans un piège électrodynamique et dans le régime optique par un mode propre d'une cavité focale de Fabry-Pérot. Pour la commande de la fréquence à long terme, les résonances d'ions piégés isolés sont des discriminateurs de précision supérieure, bien que la fréquence commandée montre des fluctuations aléatoires dues au bruit affectant le signal de rétroaction. La contribution fondamentale de l'article est le bruit quantique de projection. La détection de la fluorescence pour la génération de la rétroaction est incompatible avec les ions préparés dans un état de superposition à partir de l'excitation par l'onde émise depuis l'oscillateur. Les tentatives pour contourner cette limitation en préparant des ensembles d'ions corrélés préalablement à la mesure (la compression de spin) sont présentées.

Mots clés : Etalon fréquence, Commande fréquence, Résonateur optique, Court terme, Long terme, Stabilité fréquence, Piégeage ion, Résonance multiple, Effet quantique.

Contents

- I. Introduction.
 - II. Optical cavities.
 - III. Multi-ion traps and clocks.
 - IV. Single ions.
 - V. Quantum projection noise.
 - VI. Spin squeezing.
- References (36 ref.).

I. INTRODUCTION

The measurement of time ranks among the most fundamental and venerable kinds of measurement for both

* Universität Hamburg, Institut für Laser-Physik, Jungiusstraße 9, D-20355 Hamburg, Germany.

its practical implications and ontologic connotations [1]. Clocks count periods of invariant periodic motion. While the stability of the periodic motion of cosmic bodies has to be relied upon, when these periods are decided to define the time scale, man-made oscillators have used feedback in order to control an oscillator's phase and frequency by applying a synchronous drive. Pendulum clocks, quartz oscillators and cesium atomic clocks likewise work along this principle. The more compact and simple the reference of phase or frequency, the better it is potentially screened from ambient perturbations that shift the mean frequency of the controlled oscillator or make its phase fluctuate. It is the technical level of an epoch that determines how fundamental a reference may suffice for controlling the clock at the aspired level of phase stability.

Quantitative ways of evaluating the clock's stability include spectral and temporal analysis of its frequency and phase noise, in particular the determination of the frequency variance σ_y^2 by two-time probing and the characterization of the random variation by the pair variance [2]. These observations have revealed a few typical features of feedback-controlled oscillators:

— noise characteristics differ on long and short time scales. Thus, separate control circuits and feedback signals corresponding to these different time scales are required for efficient noise reduction;

— feedback is derived from detection of the output signal of a discriminant. The intrinsic phase and frequency uncertainty is caused, in the short-time regime, by shot noise. It is characterized by the standard deviation of the oscillator frequency

$$(1) \quad \sigma_y = \frac{1}{Q(S/N)_0 \sqrt{\tau/\tau_0}},$$

where $Q = \omega_0/\gamma$ is the quality of the controlling frequency discriminant, an atomic Lorentzian line, e.g., ω_0 and γ are its centre frequency and width, respectively, $(S/N)_0$ is the signal-noise ratio averaged over the time τ_0 , and τ is the temporal separation of two individual measurements [3]. Quantum noise limits phase stability on a short or medium time scale, when technical noise has been eliminated. On a long time scale, $1/f$ noise takes over, or low-frequency drifts whose spectrum is specified by certain dynamical features of the particular realization of the reference, e.g., from migration and relaxation of dislocations in crystals.

For application as the controlling frequency discriminant, atomic or molecular internal resonances are qualified, in principle, for their intrinsic invariability and general accessibility. The official frequency standard of many years, the cesium atomic clock, refers to the ground-state hyperfine transition of the cesium atom [1]. Controlling the phase of a microwave oscillator in the short-time regime requires a low-noise feedback signal that may be derived from the ensemble of the microwave-interacting atoms by laser-inducing and detecting the atoms' resonance fluorescence in the microwave-optical double-resonance scheme [4]. One

represents the atomic ensemble by low-density vapour in a cell filled with buffer gas, or better by an atomic beam. Also, the groundstate hyperfine transitions of ions stored as a cloud in a trap have been used as the reference. Although the strength of the feedback signal derived from an atomic or ionic line discriminant is satisfactory, an ensemble, and certainly one that consists of trapped ions, is prone to intrinsic systematics from incomplete control of the ambient conditions to which the individual members are subjected. In particular, the differing locations of the individual particles in presence of amplitude or phase gradients of the ambient fields give rise to frequency shifts which limit the reproducibility of measurements, i.e. the temporal stability.

In spite of these problems, electrodynamic traps holding some 10^6 ions do very well in the rf and microwave regime [5-8]. They are less competitive, however, for short-term frequency stabilization of optical frequencies, with focal Fabry-Pérot resonators. Although the spectral resonances of such a device are not universal, they are equally spaced and combine sharpness, i.e. high Q values, with excellent signal-noise ratio of the feedback signal. Thus, an ideal trap-based frequency standard is composed of i) an oscillator represented by an rf synthesizer or a frequency-tunable phase-stable single-mode laser, ii) a high-finesse optical cavity, or a multi-ion trap, for short-term phase and frequency control of the oscillator, and iii) a single-ion trap that provides long-term frequency control for the elimination of slow fluctuations and drifts (Fig. 1). We shall assume that the actual control is effective for time intervals longer than a few microseconds, and that the $1/f$ -noise intrinsic to the oscillator does not show up on the time scales of interest, say, up to 10^4 s. When we want to outdo current Cs atomic clocks, the frequency instability should not exceed 10^{-15} . On the other hand, high stability is prerequisite for utilizing the superior accuracy of single-ion frequency representation whose residual inaccuracies may not exceed one part in 10^{18} [9].

II. OPTICAL CAVITIES

A focal optical cavity is made up by two spherical mirrors facing each other at the fixed distance d such that the phase of a light wave of frequency $\nu = \nu_q$ reproduces after a round trip if $2nd\nu/c$ is an integer q , where n is the index of refraction between the mirrors. The resonances ν_q of the cavity are spectrally spaced by $\Delta\nu = c/2nd$. Confocal cavities ($2f = d$, e.g., where f is the common focal length of the mirrors) fulfil a resonance condition for phase reproduction perpendicular to the cavity axis whose resonance values are degenerate and interspaced between the above resonances of the longitudinal cavity modes, such that $\Delta\nu_{\text{conf}} = c/4nd$ holds [10]. The shape of these reso-

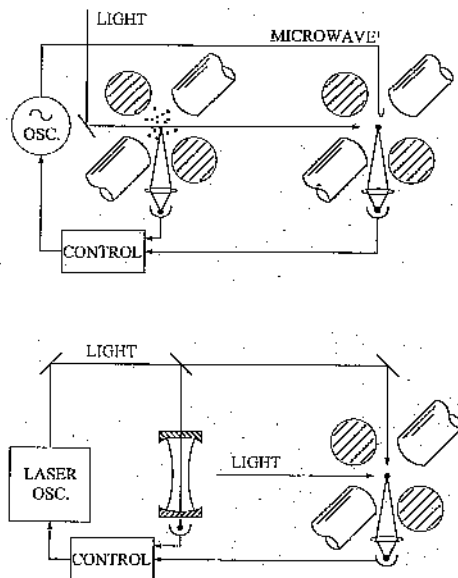


FIG. 1. — Schematics of a frequency standard based on a single ion.

Top : A microwave oscillator short-term frequency-controlled by resonance fluorescence from a cloud of ions in an electrodynamic trap, and long-term controlled by fluorescence from a single ion. Bottom : A laser oscillator whose short-term frequency stability is provided by a resonance of an optical cavity.

Schéma d'un étalon de fréquence à ion unique.

En haut : un oscillateur microondes dont la fréquence à court terme est commandée par la résonance de fluorescence d'un nuage d'ions dans un piège électrodynamique, et dont la fréquence à long terme est commandée par la fluorescence d'un ion unique. En bas : un oscillateur laser dont la stabilité de fréquence à court terme est fournie par une résonance d'une cavité optique.

nances is essentially represented by the Airy function of the transmission of a (flat) Fabry-Pérot etalon, and their finesse $F = 2\pi\Delta\nu/\gamma$, where $\gamma/2\pi$ is the full width at half maximum, may exceed 10^5 when the mirrors are coated with advanced dielectric multi-layers [11]. Controlling the oscillator frequency by 10^{-15} , is by better than 1 Hz in the optical domain. A cavity as large as the earth, when expanded by a hair's width, would shift the frequency by intolerable 300 Hz. Consequently, scrutiny of all possible sources of length shifts and fluctuations is indispensable. The foremost of these perturbations of a typical cavity ($F = 10^5$) whose mirrors are supported by a spacer rod of glass ceramics $d = 30$ cm long, and of 4 kg mass, are listed here, according to J. Bergquist *et al.* [11] :

i) Quantum fluctuations of the light, and the corresponding shot noise of light pressure, would make the cavity length d fluctuate. While the strength of the noise varies as the square root of the photon number N accumulated during the time of a measurement, the standard deviation of frequency determination decreases by $1/\sqrt{N}$. With unit detection efficiency, the optimum value of the fractional uncertainty of d is found $5 \times 10^{-22} \text{ m } \sqrt{\Delta f/\text{Hz}}$ at 3 W input power, where Δf is the frequency bandwidth of the detection. Thus with a typical $100 \mu\text{W}$ control signal quantum fluctuations do not contribute at the 10^{-15} level.

ii) The $100 \mu\text{W}$ input power to the cavity generates some 3 W intracavity flux, resulting in a light force acting onto the centres of the mirrors, which deflects the mirrors to the effect of 10^{-15} fractional change of d , or 0.5 Hz frequency variation. This effect imposes significant restrictions to the level of stabilization of the light flux (which must not vary in excess of 10% for 1 mW input, *e.g.*). In contrast, expansion of the spacer turns out to contribute on the order of negligible 10^{-17} only.

iii) Absorption of light that takes place even in the low-loss mirror coatings gives rise to local heating. Frequency shifts up to 20 Hz per μW of light input to the cavity have been observed. This problem, and also the effect of radiation pressure, may be relieved by increasing the cross section of the light beam impinging on the mirrors.

iv) The thermal noise in the spacer has been estimated to contribute, at 300 K, a mean variation of $\Delta d \approx 2 \times 10^{-15} \text{ m}$ corresponding to some 1 Hz frequency excursion at the fundamental vibration mode of the cavity rod, which is $\omega_0/2\pi \approx 10 \text{ kHz}$. However, with an actual time of measurement τ smaller than the decay time of the fundamental vibrational mode, $\tau_0 = 2Q_m/\omega_0 = 10 \text{ s}$, where Q_m is the fractional energy loss per vibrational cycle, that variation is reduced by τ/τ_0 . Thus, for suitable duration of the measurements, thermal noise has little effect to the frequency stability.

v) Thermal expansion is $10^{-8}/\text{K}$ and would require temperature control on the micro-Kelvin level. Since the cavity rod is suspended in vacuum, the coupling with the environment is mainly radiative with a long relaxation time. Temperature variations that do not exceed 10 mK will thus induce frequency drifts not exceeding 1 Hz/s.

vi) Fluctuations of the residual pressure will induce corresponding variations of the strain in the spacer rod that gives rise to $\Delta\nu/\nu \approx 10^{-16}$. However, the corresponding variation of the index of refraction is $n - 1 \approx 3 \times 10^{-9} \text{ p/Pa}$ which yields 15 Hz shift at $p = 10^{-5} \text{ Pa}$, and 1.5 Hz variation with 10% pressure fluctuations.

vii) The most serious perturbation is traced back to ambient vibrations including micro-seismic activity. While the cavity may be isolated against high-frequency components by a support consisting of shock-absorbing sheets sandwiched between passive masses, low-frequency noise requires specific attention. Pendulum suspension isolates against horizontal vibration, and spring-loaded suspension provides vertical isolation; both must be suitably damped. These suspensions may be designed as to eliminate variations of the cavity length that exceed 10^{-15} . However, the points of support in general do not perfectly match the distributed weight of the cavity rod, giving rise to strain in the rod and its support, and to corresponding deformation. This problem may be relieved by suspension in the nodal points of the vibrational modes of the cavity most subjected to excitation.

The laser oscillator is frequency-locked to a resonance of the cavity by the Pound-Drever method [12]. The light is phase-modulated, reflected off the cavity, detected, and demodulated. The resulting feedback signal, used for frequency shifting the laser oscillator, is antisymmetric as a function of its detuning from the cavity resonance, and it shows a steep linear discriminant on resonance. Over a range on the order of the modulation frequency the signal is negative for positive detuning and vice versa, such as to provide feedback even for substantial sudden excursions of the laser frequency. The fidelity of locking is as high as to routinely limit the mean laser offset from the cavity resonance to the sub-Hertz level.

III. MULTI-ION TRAPS AND CLOCKS

When a universal natural resonance is preferred as the discriminant, the numerous narrow lines of a molecular gas may do (I_2 , Te_2), or an atomic vapour in a cell immersed in background gas, or an atomic beam. However, the absolute value of the oscillator frequency determined by the discriminant is usually uncertain to the extent of line shifts by atomic collisions and ambient fields. An alternative reference is an ensemble of, say, 10^6 ions in an electrodynamic trap. Unlike with a metal vapour in a cell, there is no background gas. Unlike with an atomic beam, the ion ensemble is confined in the interaction region for unlimited time, and transit-time line broadening does not take place. However, in the optical regime, the lines of this ensemble are inhomogeneously broadened and shifted since ions in different locations in the field of trap and space charge perceive different fields, and the individual ions move with a different amplitude of their micro-motion driven by the trap drive. Each ion class of equal projection of velocity on the direction of light propagation shows time-varying Doppler shift of different frequency excursion that also limits the interaction time via the modulated spectral overlap of light and line. Still, nonlinear optical spectroscopy has derived narrow resonances (Lamb dips, electronic Raman resonances) providing discriminants that are reasonably free of uncontrolled or non-quantifiable perturbation [13].

In fact, multi-ion traps seem best qualified for frequency control in the microwave regime where Doppler effects are insignificant. An electrodynamic trap of Paul type (Fig. 2) consists of a ring electrode and two electrically connected cap electrodes. A radio-frequency voltage between ring and caps generates an ac field, with a saddle point in the centre, whose amplitude increases with the distance from the centre, and which drives the vibrating ions. The ions' kinetic energy of the driven micro-motion may be considered the potential of their free motion in the trap, the secular motion. This potential is superimposed by the space charge of the ion cloud

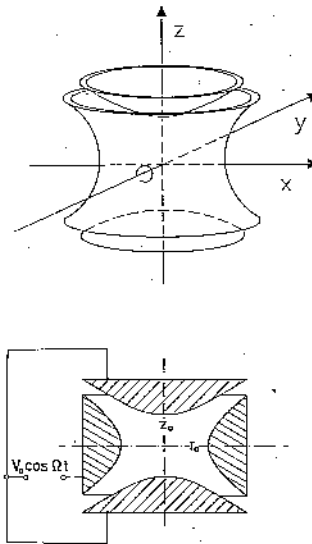


FIG. 2. — Scheme of an electrodynamic (Paul) ion trap.

Schéma du piège ionique électrodynamique (dit de Paul).

and ambient parasitic spatially inhomogeneous electric and magnetic fields, which may be partially compensated by multipolar dc fields from extra electrodes. Typical clock lines are the ionic ground-state hyperfine transitions $F = 0 \rightarrow 1$, $m_F = 0 \rightarrow 0$, which show no linear Zeeman effect and thus are insensitive to magnetic field fluctuations and field inhomogeneity. Frequency standards have been demonstrated using the corresponding lines of Ba^+ [5], Hg^+ [6], and Yb^+ [7, 14]. Here, the feedback signal is derived from an rf-optical double resonance measurement [4]: laser-excited resonance scattering yields many optical photons per individual excitation of an ion on the hyperfine clock transition, when probing takes place on a cycling resonance line (Fig. 3).

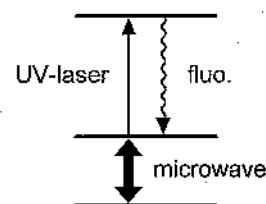


FIG. 3. — Microwave-optical double resonance scheme.

Schéma de la double résonance microonde-optique.

Let us briefly model a double-resonance measurement: pulsed interaction with the signal wave, i.e. the microwave radiation, is followed by probing one of the energy levels with resonant light scattering. There may be one signal pulse that has pulse area π on resonance, and less elsewhere (*Rabi resonance*), or two pulses of area $\pi/2$ on resonance (*Ramsey resonance*). The cohe-

rent evolution of each of the ions at the clock frequency obeys the equation of the spinning top :

$$(2) \quad d\mathbf{J}/dt = \boldsymbol{\omega}' \times \mathbf{J},$$

in a coordinate system rotating at frequency ω , where \mathbf{J} is the vector of angular momentum ($J = 1/2$, $|\mathbf{J}| = \hbar\sqrt{J(J+1)}$), and $\boldsymbol{\omega}' = (\omega_0 - \omega)\hat{z} + \omega_1\hat{y}$, where $-\mu_0 B_0/\hbar = \omega_0 - \omega_{00}$ is the Larmor frequency in the ambient dc magnetic field $B_0\hat{z}$ (ω_{00} is the resonance frequency in zero field), and $\omega_1 = -\mu_0 B_1/\hbar$ is the Rabi nutation frequency of the ion corresponding to the amplitude B_1 of the microwave magnetic field $\hat{y}B_1 \cos \omega t$. Initially, $\langle \mathbf{J}(t=0) \rangle = \hat{z}|\langle J_z(0) \rangle|$. After N ions having interacted with the signal wave for time τ , and some have been transferred to the upper level $|+\rangle$, their fluorescence scales as :

$$(3) \quad \langle N_+(\tau) \rangle = N(\omega_1/\Omega)^2 \sin^2 \Omega\tau/2,$$

where $\Omega^2 = (\omega_0 - \omega)^2 + \omega_1^2$, with single-pulse excitation (Rabi). With double-pulse excitation (Ramsey), one finds close to resonance, $|\omega_0 - \omega| \ll \omega_1$,

$$(4) \quad \langle N_+(T) \rangle = N/2 - N\langle J_z(0) \rangle \cos(\omega_0 - \omega)T,$$

when the time T of free evolution is sandwiched between the two pulses of length $\tau \ll T$. In the case of $^{171}\text{Yb}^+$, fluorescence on the line $S_{1/2}(F=1) - P_{1/2}(F=0)$ — not quite cyclic due to spurious off-resonant $P_{1/2}(1)$ excitation — marks signal excitation on the ground-state hyperfine transition $F=0 \rightarrow 1$ at 12.6 GHz (Fig. 4). Monitoring the frequency deviation requires a sequence of measurements, and the feedback signal is derived from measurements alternating on the upper and lower wings of the line, and on-line comparison of the fluorescence yield. Rabi-type detection on some 10^6 Yb^+ ions has shown a 0.4 Hz-wide line, when the microwave oscillator was controlled by the double-resonance signal with the residual frequency instability $2 \times 10^{-11} \sqrt{s/\tau}$ [7].

A recently recorded Ramsey resonance of about hundred $^{171}\text{Yb}^+$ ions is shown in Figure 5 [15]. Also, double-resonance signals less than 10 mHz wide have

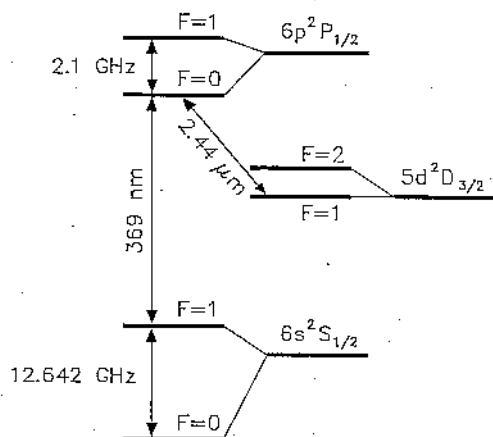


FIG. 4. — Partial level scheme of $^{171}\text{YbII}$.

Schéma partiel des niveaux pour $^{171}\text{YbII}$.

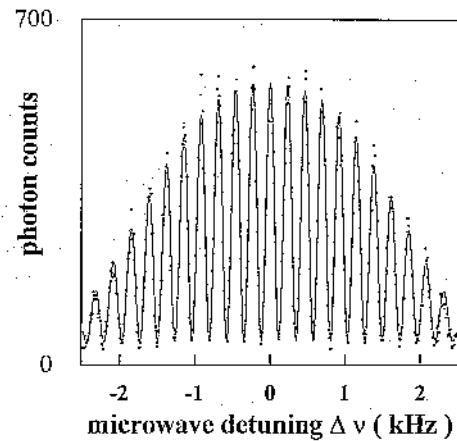


FIG. 5. — Microwave-optical double resonance signal of 100 $^{171}\text{Yb}^+$ ions in a trap, that may be used for the generation of feedback to the oscillator.

Schéma de double résonance microonde-optique pour 100 ions $^{171}\text{Yb}^+$ dans un piège, qui peut être utilisé pour la génération d'une rétroaction dans l'oscillateur.

been demonstrated with much larger clouds of $^{171}\text{Yb}^+$ ions [14]. In these measurements, the noise on the observed signals — and the potential frequency stability of a locked oscillator — is eventually limited by the shot noise of the fluorescence detection, whose overall efficiency is determined by the spatial angle of detection — less than 10% of 4π —, and by the efficiency of photon counting being well below unity.

IV. SINGLE IONS

Some years ago, the preparation, manipulation, and detection of a single ion confined in an electrodynamic trap have been demonstrated [16]. Laser cooling [17-19] makes eliminate the ion's motion and allows to localize the ion in the very node of the rf field in the centre of the trap, unlike with the Coulomb-repelling ions in a cloud. Consequently, Doppler effects and Stark shift are absent, along with transit-time line broadening, since the time of interaction with the light is effectively unlimited. While field gradients do not affect the ion, slow temporal variation of the ambient magnetic field may be allowed for by alternating measurements on symmetrically up-shifted and down-shifted Zeeman components of a line. The Stark shift by black-body radiation is well known [20] and may be corrected for.

Since the intrinsic inaccuracy of a frequency standard based on a single ion is so small, the actual frequency instability should be adequate in order to limit the duration of measurement required to represent the accurate frequency. However, the signal-noise ratio of the single ion's laser-excited fluorescence is restricted by saturation. Although quantum-limited photon counting rates on the order of $5 \times 10^4/\text{s}$ have been routinely achieved, it needs an additional strategy to overcome the effect of noise on the feedback :

(i) Dark lines as a frequency reference : the fluctuations of the controlled frequency are minimized by using a narrow nonlinear resonance as the steep frequency discriminant for the control. A line applicable for this purpose is the electronic E2 transition $S_{1/2} - D_{3/2}$ of the Ba^+ ion (Fig. 6). When two-photon excited as the frequency difference (*electronic Raman* excitation) by light at 493 nm and 650 nm, close to one-photon resonance lines $S_{1/2} - P_{1/2}$ and $P_{1/2} - D_{3/2}$, this transition gives rise to a *dark line* [21] which is the signature of a *trapped state* [22] : optical pumping generates a coherent superposition of the S and D states that decouples from the light, cannot be excited any more, and stops scattering light. Since the $D_{3/2}$ level lives 48 s [23], the natural width of this line is 10 mHz only. A non-zero magnetic field is required in order to avoid optically pumping the ion to a Zeeman level inaccessible by the linearly polarized laser light. Four Zeeman-shifted transitions are two-photon allowed when the polarization of the light is linear and perpendicular with the magnetic field, namely $m_J(S_{1/2}) = \pm 1/2 \rightarrow m_J(D_{3/2}) = \pm 1/2, \mp 3/2$. They form dark lines which show up in an excitation spectrum of a Ba^+ ion's fluorescence upon scanning the red laser one of which is shown in Figure 7. The observed widths of the dark lines are mainly caused by residual power broadening. A linewidth of 10 kHz seems feasible, recorded with $S/N \approx 50$. When the red-laser oscillator were frequency-locked to one of these dark lines, the difference of green and red laser frequencies generated in a nonlinear crystal would establish a standard frequency of mean standard deviation $\sigma_y \approx 4 \times 10^{-13} \tau^{-1/2}$. So far, this approach still falls short of outperforming the precision of an up-to-date Cs clock.

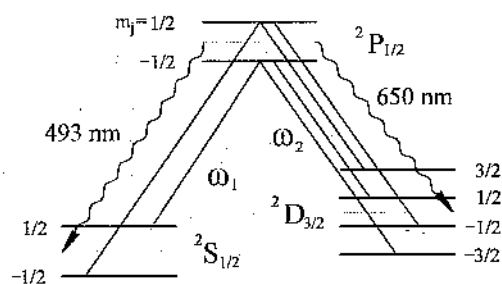


FIG. 6. — Partial level scheme of BaII including Zeeman effect.

Schéma partiel des niveaux BaII incluant l'effet Zeeman.

(ii) Opto-optical Rabi-type double resonance detected by quantum amplification : the ion may be excited by pulses of the signal wave which is laser light that matches a corresponding high- Q -clock transition, e.g. the E2 line BaII $S_{1/2} - D_{5/2}$ at $1.76 \mu m$ (Fig. 8). Possible excitation on this clock line is sequentially probed by interrogating the appearance of fluorescence on a neighbouring optical resonance line, as the BaII $S_{1/2} - P_{1/2}$ line. Present fluorescence proves, with *unit efficiency*, the ion to remain in the ground state, absent fluorescence signals the ion to be on the $D_{5/2}$

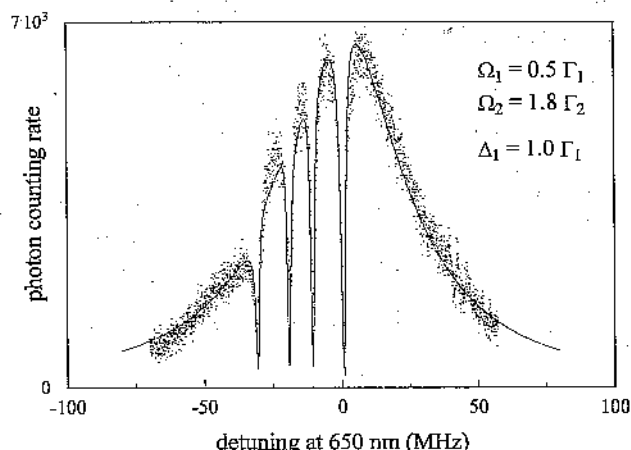


FIG. 7. — Fluorescence of single Ba^+ ion vs detuning of red laser light ("excitation spectrum").

Four *dark lines* show up that correspond to the allowed two-photon transitions $S_{1/2} (m = \pm 1/2) \rightarrow D_{3/2} (m = \pm 1/2, \mp 3/2)$.

Fluorescence d'un ion isolé Ba^+ en fonction du décalage de la lumière du laser rouge (« spectre d'excitation »).

Quatre lignes noires sont observées qui correspondent aux transitions permises à deux photons : $S_{1/2} (m = \pm 1/2) \rightarrow D_{3/2} (m = \pm 1/2, \mp 3/2)$.

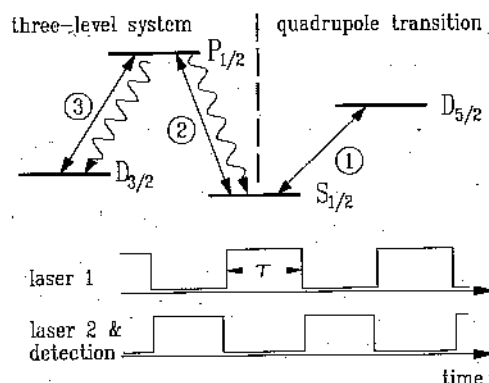


FIG. 8. — Scheme of opto-optical double resonance on a single trapped ion, making use of quantum amplification.

Lasers 1 and 2 alternate ; laser 3 (continuously on) repumps the ion from the $D_{3/2}$ metastable level. When signal laser 1 succeeds in exciting the atom to level $D_{5/2}$, subsequent pulse of laser 2 cannot excite resonance scattering on the line S - P . With laser 1 detuned from resonance by the frequency of the free ionic vibration in the trap (*secular frequency*), selected vibrational states $|n\rangle$ are accessible by side-band excitation when the ion is initially prepared in $|0\rangle$.

Schéma de la résonance double opto-optique d'un ion piégé unique qui fait usage de l'amplification quantique.

Les lasers 1 et 2 sont intermittents ; le laser 3 (en continu) repompe l'ion à partir du niveau métastable $D_{3/2}$. Lorsque le signal laser 1 réussit à exciter l'atome au niveau $D_{5/2}$, l'impulsion ultérieure du laser 2 ne peut pas exciter la résonance diffusée sur la ligne S - P . Grâce au laser 1 décalé de la résonance par la fréquence de la vibration ionique libre dans le piège (fréquence séculaire), les états de vibration sélectionnés $|n\rangle$ sont accessibles à l'excitation latérale lorsque l'ion est initialement préparé en $|0\rangle$.

level. This is in fact a *digitized* variant of the previous double-resonance scheme which is now combined with the concept of *quantum amplification* [24, 25]. When the detection cycles with zero fluorescence are accumulated, and their number is recorded vs the stepwise scanned frequency of the laser radiation, this distribution is an excitation spectrum. Such a spectrum accumulated for 130 s is shown in Figure 9; it represents the $6^2S_{1/2}(m = +1/2) \leftrightarrow 5^2D_{5/2}(m = +3/2)$ component of the E2 line. Its line shape may be used as the discriminant for controlling the oscillator frequency.

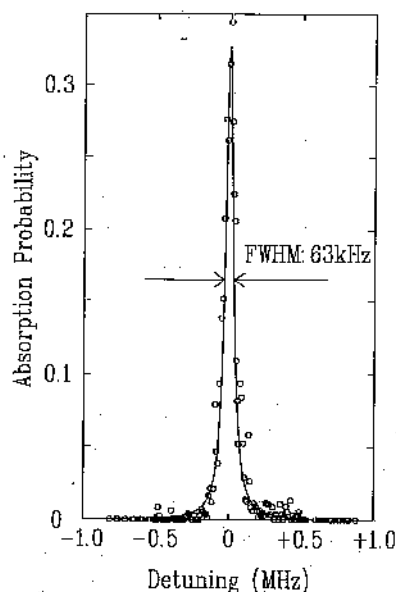


FIG. 9. — Absorption probability (normalized number of no fluorescence events) of a single cold Ba^+ ion excited on the $S_{1/2} - D_{5/2}$ E2 line at $1.76 \mu\text{m}$, vs detuning of this light from resonance. Fluorescence is excited on the $S_{1/2} - P_{1/2}$ resonance line, and red light (650 nm) prevents optical pumping into the $D_{3/2}$ state.

Probabilité d'absorption (nombre normalisé des événements sans fluorescence) d'un ion isolé froid Ba^+ excité sur la transition E2 : $S_{1/2} - D_{5/2}$ à $1.76 \mu\text{m}$ en fonction du décalage de la lumière par rapport à la résonance. La fluorescence est excitée sur la transition résonante $S_{1/2} - P_{1/2}$, et la lumière rouge (650 nm) empêche le pompage optique vers le niveau $D_{3/2}$.

Detuning the frequency to the lower wing would be made alternate with tuning to the upper wing, and from the difference of the recordings the feedback signal would be derived that controls the oscillator's mean frequency. The noise intrinsic to the frequency excursion of the oscillator is related to the readout of the ion state after coherent preparation by a pulse of signal light. Subsequent probing the appearance of fluorescence is equivalent to *projecting* the ion into one of the energy eigenstates of the signal line. With the E2 line of Ba^+ , an *on* signal projects it to the ground state $S_{1/2}$, an *off* signal to the excited state $D_{5/2}$. The detection of the energy eigenstate of the ion thus represents a measurement *incompatible* with the ion's preparation, by one pulse of signal light, in a superposition state. In general,

the recorded data of repeated measurements are distributed around the expectation value as required by quantum uncertainty. This distribution has maximum variance after dipole excitation by a $\pi/2$ pulse. The results coincide, however, if the ion had been prepared, *e.g.*, by a π pulse, in an energy eigenstate. The randomness of incompatible detection which is at the very heart of quantum mechanics, gives rise to fluctuations of the outcome of sequential frequency measurements even after having identically prepared the ion.

(iii) Microwave-optical Ramsey-type double resonance detected by quantum amplification. The detection of individual acts of excitation of a single ion on the clock transition by probing the ion's fluorescence may also complement double-pulse excitation. This procedure is outlined in Figure 10, where the pulse sequences of resonantly scattered uv light, microwave signal, and photon counting are indicated. A pulse of uv light pumps the ion to the $F = 0$ ground-state. If each of the subsequent microwave pulses is a $\pi/2$ pulse, the ion will be invariably found in the upper state upon the next probing of the uv fluorescence. Otherwise, the uv light may or may not generate a burst of fluorescence to be detected by the photomultiplier. These random results which correspond to finding the ion in the state $F = 1$ or 0 , respectively, are distributed such as to reproduce the expectation value of level populations, and its variance. Detuning the microwave off resonance makes vary the expectation value $\langle N_+ \rangle$ periodically. With a large number of accumulated observations, Ramsey fringes show up. At mid-wing of a fringe, the results are equally distributed over upper and lower state, since the double-pulse excitation corresponds to a total $\pi/2$ pulse that

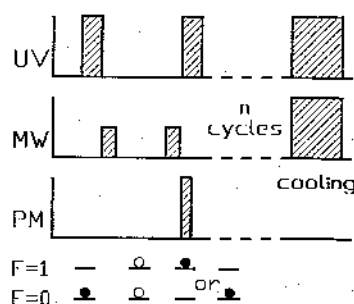


FIG. 10. — Schematics of Ramsey-type microwave-optical double resonance on single ion.

The switching sequences of the UV laser light that excites resonance scattering, of the microwave, and of the photomultiplier are shown. After n cycles, the two radiations are simultaneously switched on for optically cooling the ion. An individual measurement finds the ion in the upper or lower hyperfine state. The results are random and distributed by a binomial distribution.

Schéma de la double résonance microonde-optique de type Ramsey.

Les séquences de déclenchement correspondant à la lumière laser UV qui excite la fluorescence, à la microonde et au photomultiplicateur sont mises en évidence. Au bout de n cycles les deux rayonnements sont simultanément déclenchés pour le refroidissement optique de l'ion. Une mesure individuelle trouve l'ion dans l'état hyperfin supérieur ou inférieur. Les résultats sont aléatoires et distribués selon une distribution binomiale.

generates a dipole. It will be shown that this preparation of the ion relates to the largest possible variance of the probing results. Figure 11 shows a Ramsey spectrum of a single $^{171}\text{Yb}^+$ ion accumulated from 50 scans of the microwave frequency across the hyperfine transition.

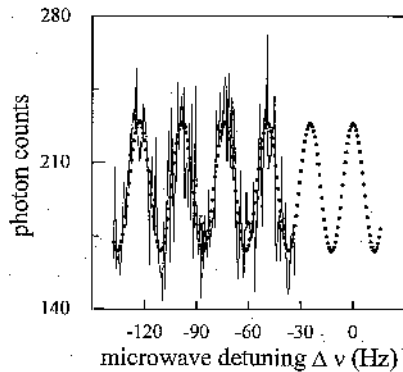


FIG. 11. — Spectrum of Ramsey-type microwave-optical double resonance ("Ramsey fringes") observed on a single trapped and cooled $^{171}\text{Yb}^+$ ion. Dots : Numerical fit. Microwave frequency at $\Delta\nu = 0$ is 12 642 815 400 Hz ($B_0 = 3211 \mu\text{T}$) which is Zeeman-upshifted from zero-field resonance at 12 642 812 118 Hz.

Spectre de la double résonance microonde-optique de type Ramsey (franges de Ramsey) observé sur un ion $^{171}\text{Yb}^+$ piégé et refroidi. Les points correspondent à une régression numérique. La fréquence microonde à $\delta\nu = 0$ de 12 642 815 400 Hz ($B_0 = 321 \mu\text{T}$) est décalée vers le haut par l'effet Zeeman à partir de la résonance en champ nul à 12 642 812 118 Hz.

V. QUANTUM PROJECTION NOISE

The fluctuations caused by the uncertainty of a quantum measurement have been analyzed by Itano *et al.* [26].

Let us assume the ion to be in state $|J = -1/2\rangle = |-\rangle$ initially. For resonant excitation ($\omega = \omega_0$) on the clock line, $|-\rangle \rightarrow |+\rangle$, the probability of finding the ion in state $|+\rangle$ is $\langle +|J_z|+\rangle = p_+ = \sin^2(\Omega T/2)$, where $\Omega = \omega_1$ since $\omega \simeq \omega_0$. In a double-resonance measurement with Ramsey detection, the spectral distribution of the probability is periodic, varies as :

$$(5) \quad p_+ = \frac{1}{2} [1 + \cos(\omega - \omega_0)T],$$

and shows maximum uncertainty at half maximum of the signal where the superposition state is prepared with equal contributions of the ground and excited states.

The width of the distribution, around p_+ , of test results finding the ion in state $|+\rangle$ is characterized by the variance of the projection operator $P_+ = |+\rangle\langle +|$:

$$(6) \quad \sigma_+^2(1) = \langle (P_+ - \langle P_+ \rangle)^2 \rangle = \langle P_+ \rangle (1 - \langle P_+ \rangle) = p_+ (1 - p_+).$$

This width is maximum for $p_+ = 1/2$, corresponding to equal superposition of states. If the trap contains $N = \langle N_- \rangle + \langle N_+ \rangle$ ions, the probability of detecting a particular value $\langle N_+ \rangle = Np_+$ is a binomial distribution whose variance is :

$$(7) \quad \sigma_+^2(N) = Np_+(1 - p_+).$$

The corresponding uncertainty of the frequency determined from the photon counting rate via the line discriminator is :

$$(8) \quad |\Delta\omega| = \sigma_+(N) / \frac{\partial \langle N_+ \rangle}{\partial \omega} = 1/T\sqrt{N},$$

since both the standard deviation σ_+ and $\partial \langle N_+ \rangle / \partial \omega$ vary, upon detuning, as $\sin(\omega - \omega_0)T$. This result holds with N uncorrelated ions, initially prepared in one of the two eigenstates of the signal transition. However, if the preparation is not known with certainty, or if there is additional noise of the detection, $\Delta\omega$ does depend on the actual detuning of the wave from the peak of the line. It is smallest for maximum slope of the line shape, *i.e.* at the half-maximum points [27].

Observations of projection noise have been reported on a single Hg^+ ion in an electrodynamic trap, and on ensembles of Be^+ ions in an electromagnetic trap [26]. In order to profit from a large ion number with minimum spurious perturbation introduced, localization of all ions in field-free positions is required. This condition is almost met by ions on the axis of a linear electrodynamic trap.

VI. SPIN SQUEEZING

One may do even better than indicated by eq. (8) when correlation is established among the N ions prior to the double-resonance measurement [27]. It is useful to describe the ions by uncorrelated angular momentum eigenstates (Dicke states) $|J, M\rangle$, where $J = N/2$, and the ground state of the system is $M = -J$. The dynamics of the ions again obeys eq. (2). The improvement is quantified by defining the squeezing parameter $\xi_R = |\Delta\omega|/|\Delta\omega_{\text{DS}}| = \Delta\varphi/\Delta\varphi_{\text{DS}} = \sqrt{2J}\Delta J_\perp/|\langle J \rangle|$, where ΔJ_\perp is the transversal standard deviation of J in the direction of rotation. The actual standard deviation of finding the state rotated by φ in configuration space, $\Delta\varphi = \Delta J_\perp/|\langle J \rangle|$, is compared with the analogous standard deviation $\Delta\varphi_{\text{DS}} = (2J)^{-1/2}$ of a rotated Dicke state. A Dicke state describes uncorrelated ions which remain uncorrelated irrespective of the rotation, *i.e.* after the application of the Ramsey pulses. This squeezing parameter measures the sensitivity to rotation in the configuration space. It is :

$$(9) \quad \xi_R = \sqrt{2J}\Delta J_z(t_f)/|\langle J_y(t_f) \rangle| = \sqrt{2J}\Delta J_y(0)/|\langle J_z(0) \rangle|,$$

when the ions start in the state $|J, -J\rangle$ at time zero, the rotation is about the x -axis, and t_f is the duration of the measurement, *i.e.* the time after the second pulse. A large value of $\langle J_z(0) \rangle$ and a narrow distribution ΔJ_y in the direction of rotation result in the desired small ξ_R . Since best correlation yields $|\Delta\omega| = 1/TN$, the squeezing parameter has a lower boundary, $\xi_R \geq 1/\sqrt{N}$. The standard deviation of frequency corresponding to the smallest value of ξ_R improves, upon increased ion number, as N^{-1} instead of $N^{-1/2}$, admitting a substantial gain of precision of the frequency control.

As for the representation of particular correlated states and ways of generating them, we summarize here results of Wineland *et al.* [27, 28].

Suitable correlations of two ions ($N = 2$, $J = 1$) have been found to be described by the initial state :

$$(10) \quad \psi(0) = (2 \cosh 2\theta)^{-1/2} (e^{-\theta} |+\rangle_1 |+\rangle_2 + e^{\theta} |-\rangle_1 |-\rangle_2),$$

which is the special case $J = 1$, $M = 0$ of :

$$(11) \quad \psi(J, M, \theta) = C_J \exp(-\theta J_z - i\pi J_x/2) |J, M\rangle,$$

[29]. For $\theta \rightarrow \infty$, this is $|1, -1\rangle$ with $\xi_R \simeq 1$, but in the limit $\theta \rightarrow 0$, $\xi_R \simeq 1/\sqrt{N} = 1/\sqrt{2}$, *i.e.* this state allows optimum squeezing. It is transformed, by the interaction with the Ramsey pulses, into the entangled state :

$$(12) \quad \psi(t_f) = 2^{-1/2} (|+\rangle_1 |-\rangle_2 + |-\rangle_1 |+\rangle_2),$$

which is characterized by correlation of the EPR type [30]. The entanglement indicates why the uncertainty of the outcome of a measurement is reduced. The mean value of the upper-level population $\langle N_+(t_f) \rangle$ of the state of eq. (10) is shown in Figure 12 in comparison with the uncorrelated Dicke state $|1, -1\rangle$. Note that at the total Ramsey phase shift $\pi/2$, which characterizes excitation on the wing of a fringe, the uncertainty of frequency, $|\Delta\omega|$, is reduced!

Although identifying states of minimum ξ_R is not straightforward for $N > 2$, the states of eq. (11) have been shown to allow minimum values of the squeezing parameters $1 > \xi_R > 1/\sqrt{N}$ for $N > 2$ [31].

A correlated spin system may be generated by coupling the system to a *squeezed harmonic oscillator* followed by transfer of the squeezing by radiative interaction via electronic Raman excitation. This coupling is described by a Jaynes-Cummings Hamiltonian whose oscillator usually represents a field mode. However, the JC Hamiltonian may also describe the harmonic centre-of-mass motion of the trapped ions coupled to their internal excitation that is represented by the spin system [32]. More specific, the harmonic oscillator may represent a mode of collective vibration of N ions arranged along the nodal line of a linear trap, which is mediated by the Coulomb repulsion of the ions. Let us assume that the collective ion vibration has been manipulated such as to show reduced uncertainty in one quadrature of its phase space. Irradiating the ions with light pulses of area $\Omega_i t$

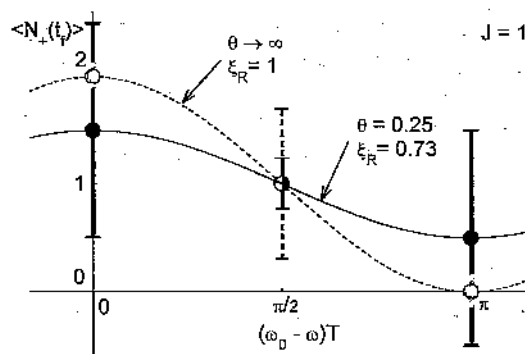


FIG. 12. — Spin squeezing.

Mean population $\langle N_+(t_f) \rangle$ of state $|+\rangle$ after second pulse at $t_f = t + 2\tau$, vs $(\omega_0 - \omega)T$, and σ_+ (bars), for ion initially in $\psi(0)$ (eq. 10). Dashed line : $\theta \rightarrow \infty$, $\psi(0) \rightarrow |1, -1\rangle$, $\sigma_+ \rightarrow 0$ at $\delta\omega = \omega_0 - \omega = 0$, π/T since corresponding $\psi(t_f)$ is energy eigenstate $|1, 1\rangle$, $|1, -1\rangle$, respectively. However, $\partial\langle N_+ \rangle / \partial\delta\omega \sim \sigma_+$, and $|\Delta\omega|$ (eq. 8) does not improve. Full line : Ions correlated; $\theta = 1/4$; here σ_+ , ξ_R , and $|\Delta\omega|$ are reduced at $\delta\omega = \pi/2T$, but increased at 0, π/T . After D. J. Wineland *et al.* [28].

Compression de spin.

Population moyenne $\langle N_+(t_f) \rangle$ du niveau $|+\rangle$ après la deuxième impulsion à $t_f = t + 2\tau$ en fonction de $(\omega_0 - \omega)T$ et σ_+ (barres) pour l'ion initialement en $\psi(0)$ (eq. 10). Ligne en pointillés : $\theta \rightarrow \infty$, $\psi(0) \rightarrow |1, -1\rangle$, $\sigma_+ \rightarrow 0$ à $\delta\omega = \omega_0 - \omega = 0$, π/T puisque le $\psi(t_f)$ correspondant est un état propre d'énergie $|1, 1\rangle$, $|1, -1\rangle$, respectivement. Cependant, $\partial\langle N_+ \rangle / \partial\delta\omega \sim \sigma_+$, et $|\Delta\omega|$ (eq. 8) n'améliore pas. Ligne en traits pleins : ions corrélés ; $\theta = 1/4$; ici σ_+ , ξ_R , et $|\Delta\omega|$ sont réduits à $\delta\omega = \pi/2T$, mais accrus à 0, π/T (d'après D. J. Wineland *et al.* [28]).

on the first vibrational sideband may transfer the squeezing to the internal degree of freedom. From a perturbative solution of the Heisenberg equations of motion, the parameters of the oscillation's squeezing, ξ_x , and of spin squeezing, ξ_R are found to obey :

$$(13) \quad \xi_R^2(t) = \cos^2 \sqrt{N}\Omega_i t + \xi_x^2(0) \sin^2 \sqrt{N}\Omega_i t,$$

where Ω_i is the Rabi frequency of the radiative interaction used for the transfer, and ξ_x is the squeezing parameter that characterizes the preparation of the ions in a squeezed vibrational state. Thus, for optimized pulse area, ξ_R varies in proportion with ξ_x . Numerical calculations reveal, however, that the resulting ξ_R turns large again for ξ_x approaching small values, *i.e.* the transfer is inefficient with small vibrational squeezing. Still, $\xi_R < 0.5$ may be achieved with $J > 10$ ($N > 20$). On the other hand, these calculations show that $\xi_R < 1$ may result even from coupling to a non-squeezed oscillator in a *coherent* state. Moreover, replacing pulsed preparation by cw interaction at twice the frequency of vibration may result in parametric pumping of squeezed vibration and transfer of that squeezing to the spin system.

The implementation of this complex program requires, first, to prepare states of trapped ions in coherent or squeezed states of their vibrational motion. This step has been implemented very recently, at the National Institute for Science and Technology (Boulder, Colo.), by laser-stimulated Raman excitation of vibrational sidebands to the groundstate hyperfine transition of a $^9\text{Be}^+$ ion [33]. Vibrational Fock, coherent, and squeezed states

have been demonstrated. Alternatively, the ion vibration may be manipulated by driving a narrow optical transition on a sideband generated from modulation by the centre-of-mass motion. At Hamburg University, a single $^{138}\text{Ba}^+$ ion has been laser-excited on these vibrational sidebands of the E2 line $S_{1/2} - D_{5/2}$, in order to establish the JC coupling to the ion vibration. So far, a vibrational Fock state seems to have been prepared [34]. Although efficient transfer of squeezing to the collective spin of a multi-ion ensemble remains to be demonstrated, these results seem encouraging. They show that quantum projection noise is not supposed to remain a fundamental limitation to high-precision frequency measurement and control, when using a narrow line of correlated ions in a trap as the frequency discriminant.

Noise reduction is not the only subject expected to benefit from the generation of correlated states and spin squeezing in well-defined ensembles of ions confined in a trap. Such correlated ensembles have been found useful for the implementation of gates for quantum computing [35, 36]. The analysis of projection noise in these prospective devices will need and justify particular attention.

Manuscrit reçu le 22 mai 1996.

REFERENCES

- [1] ***. Frequency standards and metrology. A. de Marchi, ed., Springer-Verlag, Berlin (1989).
- [2] ALLAN (D. A.). Statistics of atomic frequency standards. *Proc. IEEE* (1966), **54**, p. 221.
- [3] VANIER (J.), AUDOIN (C.). The quantum physics of atomic frequency standards. IOP Publishing Ltd., London (1989).
- [4] KASTLER (A.), BROUSSEL (J.). The detection of magnetic resonance of excited levels : depolarization effect of optical resonance and fluorescence radiations. *C.R. Acad. Sci.* (1949), **229**, p. 1213. BROUSSEL (J.), BITTER (F.). A new 'double resonance' method for investigating atomic energy levels. Application to $\text{Hg}^3 \text{P}_1$. *Phys. Rev.* (1952), **86**, p. 308.
- [5] BOLLINGER (J. J.), WALLS (J. S.), WINELAND (D. J.), ITANO (W. M.). Hyperfine structure of the $2p^2 \text{P}_{1/2}$ state in ^9B . *Phys. Rev. A* **31** (1985), p. 2711. BOLLINGER (J. J.), PRESTAGE (J. D.), ITANO (W. M.), WINELAND (D. J.). Laser-cooled atomic frequency standard. *Phys. Rev. Lett.* (1985), **54**, p. 1000.
- [6] CUTLER (L. S.), FLORY (C. A.), GIFFARD (R. P.), MCGUIRE (M. D.). Doppler effects due to thermal macromotion of ions in an rf quadrupole trap. *Appl. Phys. B* **39** (1986), p. 251.
- [7] CASDORFF (R.), ENDERS (V.), BLATT (R.), NEUHAUSER (W.), TOSCHEK (P. E.). A 12-GHz standard clock on trapped ytterbium ions. *Ann. Phys.*, Leipzig (1991), **48**, p. 41.
- [8] JARDINO (M.), DESAINTEUSCEN (M.), BARILLET (R.), VIENNET (J.), PETIT (P.), AUDOIN (C.). Frequency stability of a mercury ion frequency standard. *Appl. Phys.* (1981), **24**, p. 107.
- [9] WINELAND (D. J.), ITANO (W. M.), BERGQUIST (J. C.), BOLLINGER (J. J.), DIEDRICH (F.), GILBERT (S. L.). High accuracy spectroscopy of stored ions. A. de Marchi, ed., Springer-Verlag, Berlin (1989).
- [10] SIEGMAN (A. E.). Lasers. University Science Books, Mill Valley, Cal. (1986).
- [11] BERGQUIST (J. C.), ITANO (W. M.), WINELAND (D. J.). Laser stabilization to a single ion. *Proc. Int. School of Phys. E. Fermi CXX*, North Holland (1994), p. 359.
- [12] POUND (R. V.). Electronic frequency stabilization of microwave oscillators. *Rev. Sci. Instr.* (1946), **17**, p. 490. DREYER (R. W. P.), HALL (J. L.), KOWALSKI (F. V.), HOUGH (J.), FORD (G. M.), MUNLEY (S. J.), WARD (H.). Laser phase and frequency stabilization using an optical resonator. *Appl. Phys. B* (1983), **31**, p. 97.
- [13] SCHUBERT (M.), SIEMERS (I.), BLATT (R.). Line shape of three-level ions in Paul traps. *Phys. Rev. A* (1989), **39**, p. 5098.
- [14] TAMM (C.), SCHNIER (D.), BAUCH (A.). Radio-frequency laser double-resonance spectroscopy of trapped ^{171}Yb ions and determination of line shifts of the ground-state hyperfine resonance. *Appl. Phys. B* (1995), **60**, p. 19.
- [15] HUESMANN (R.), COURTEILLE (P.), NEUHAUSER (W.), TOSCHEK (P. E.). Ramsey fringes of a single cold $^{171}\text{Yb}^+$ ion. To be published.
- [16] NEUHAUSER (W.), HOHENSTATT (M.), TOSCHEK (P. E.), DEHMELT (H.). Localized visible Ba^+ mono-ion oscillator. *Phys. Rev. A* (1980), **22**, p. 1137.
- [17] NEUHAUSER (W.), HOHENSTATT (M.), TOSCHEK (P. E.), DEHMELT (H. G.). Visual observation and optical cooling of electrostatically contained ions. *Appl. Phys.* (1978), **17**, p. 123.
- [18] NEUHAUSER (W.), HOHENSTATT (M.), TOSCHEK (P. E.), DEHMELT (H. G.). Optical sideband cooling of visible atom cloud confined in parabolic well. *Phys. Rev. Lett.* (1978), **41**, p. 233.
- [19] WINELAND (D. J.), DRULLINGER (R. E.), WALLS (F. L.). Radiation-pressure cooling of bound resonant absorbers. *Phys. Rev. Lett.* (1978), **40**, p. 1639.
- [20] HOLLBERG (L.), HALL (J. L.). Measurement of the shift of Rydberg energy levels induced by blackbody radiation. *Phys. Rev. Lett.* (1984), **53**, p. 230.
- [21] SIEMERS (I.), SCHUBERT (M.), BLATT (R.), NEUHAUSER (W.), TOSCHEK (P. E.). The 'trapped state' of a trapped ion - line shifts and shape. *Europhys. Lett.* (1992), **18**, p. 139. HÄNSCH (T.), TOSCHEK (P. E.). Theory of a three-level gas laser amplifier. *Z. Phys.* (1970), **236**, p. 213.
- [22] ALZETTA (G.), GOZZINI (A.), MOI (L.), ORRIOLS (G.). An experimental method for the observation of rf transitions and laser beat resonances in oriented Na vapour. *Nuovo Cimento B* (1976), **36**, p. 5.
- [23] KNAB-BERNARDINI (C.), KNAB (H.), VEDEL (F.), WERTH (G.). Experimental lifetime of the metastable $5 \text{D}_{3/2}$ in Ba. *Z. Phys.* **D** (1992), **24**, p. 339.
- [24] NAGOURNEY (W.), SANDBERG (J.), DEHMELT (H.). Shelved optical electron amplifier : observation of quantum jumps. *Phys. Rev. Lett.* (1986), **56**, p. 2797.
- [25] SAUTER (T.), NEUHAUSER (W.), BLATT (R.), TOSCHEK (P. E.). Observation of quantum jumps. *Phys. Rev. Lett.* (1986), **57**, p. 1696.
- [26] ITANO (W. M.), BERGQUIST (J. C.), BOLLINGER (J. J.), GILLIGAN (J. M.), HEINZEN (D. J.), MOORE (F. L.), RAIZEN (M. G.), WINELAND (D. J.). Quantum projection noise : population fluctuations in two-level systems. *Phys. Rev. A* (1993), **47**, p. 3554.
- [27] WINELAND (D. J.), BOLLINGER (J. J.), ITANO (W. M.), MOORE (F. L.). Spin squeezing and reduced quantum noise in spectroscopy. *Phys. Rev. A* (1992), p. 6797.
- [28] WINELAND (D. J.), BOLLINGER (J. J.), ITANO (W. M.), HEINZEN (D. J.). Squeezed atomic states and projection noise in spectroscopy. *Phys. Rev. A* (1994), **50**, p. 67.
- [29] RASHID (A.). The intelligent states. I. Group-theoretic study and the computation of matrix elements. *J. Math. Phys.* (1978), **19**, p. 1391. AGARWAL (G. S.), PURI (R. R.). Cooperative behavior of atoms irradiated by broadband squeezed light. *Phys. Rev. A* (1990), **41**, p. 3782.
- [30] EINSTEIN (A.), PODOLSKY (B.), ROSEN (N.). Can quantum-mechanical description of physical reality be considered complete? *Phys. Rev.* (1935), **47**, p. 777. BOHM (D.). Quantum theory. Prentice-Hall, Englewood Cliffs, NJ (1951), p. 611.
- [31] AGARWAL (G. S.), PURI (R. R.). Atomic states with spectroscopic squeezing. *Phys. Rev. A* (1994), **49**, p. 4968.
- [32] BLOCKLEY (C. A.), WALLS (D. F.), RUSKEN (H.). Quantum collapses and revivals in a quantized trap. *Europhys. Lett.* (1992), **7**, p. 509.
- [33] MEEKHOF (D. M.), MONROE (C.), KING (B. E.), ITANO (W. M.), WINELAND (D. J.). Generation of nonclassical motional states of a trapped atom. *Phys. Rev. Lett.* (1996), **76**, p. 1796.
- [34] APPASAMY (B.), STALGIES (Y.), TOSCHEK (P. E.). Contributions to the implementation of a single-ion frequency standard. *Proceedings of the Colloquium 'Frequenznormale mit laserpräparierten Atomen und Ionen'*, Deutsche Forschungsgemeinschaft, Schierke, Oberharz (12-14 Feb. 1996).
- [35] CIRAC (J. J.), ZOLLER (P.). Quantum computations with cold trapped ions. *Phys. Rev. Lett.* (1995), **74**, p. 4091.
- [36] MONROE (C.), MEEKHOF (D. M.), KING (B. E.), ITANO (W. M.), WINELAND (D. J.). Demonstration of a fundamental quantum logic gate. *Phys. Rev. Lett.* (1995), **75**, p. 4714.